Renewable Energy 223 (2024) 120018

Contents lists available at ScienceDirect

Renewable Energy

journal homepage: www.elsevier.com/locate/renene

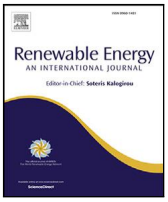

An Ocean Thermal Energy Conversion power plant: Advanced exergy analysis and experimental validation

Dario Colorado-Garrido [a,*], Emmanuel Mendoza-Bernal [b], Lili M. Toledo-Paz [b], Beatris A. Escobedo-Trujillo [c]

[a] Centro de Investigación en Recursos Energéticos y Sustentables (CIRES), Universidad Veracruzana, Av. Universidad Veracruzana Km. 7.5, Col. Santa Isabel I, Coatzacoalcos, 96538, Veracruz, Mexico
[b] Maestría en Ciencias en Tecnología Energética (MaCTE), Centro de Investigación en Recursos Energéticos y Sustentables (CIRES), Universidad Veracruzana, Av. Universidad Veracruzana Km. 7.5, Col. Santa Isabel I, Coatzacoalcos, 96538, Veracruz, Mexico
[c] Facultad de Ingeniería, Universidad Veracruzana, Av. Universidad Veracruzana Km. 7.5, Col. Santa Isabel I, Coatzacoalcos, 96538, Veracruz, Mexico

ARTICLE INFO

Keywords:
Avoidable endogenous
Dry refrigerant
Ammonia
Organic rankine cycle
Jacob number

ABSTRACT

An ocean thermal energy conversion power plant was simulated from the point of view of the first, the second law of thermodynamics, and advanced exergy analysis with the aim of increasing the efficiency of the cycle, quantifying and knowing the nature of the exergy destruction. First, the net power output and efficiency of the cycle were successfully calculated as a function of the surface temperature and a certain depth of the ocean, given a pinch temperature differential and the mass flow of seawater in the evaporator and condenser. The numerical simulation are compared with experimental evidence, obtaining better results than thermodynamic models previously reported. Then, the second law of thermodynamics analysis was made using appropriate correlations for the estimation of thermo-physical properties of seawater, revealing the imprecision of assuming properties of pure water in the calculation of the total exergy destruction of the system. Finally, advanced exergy analysis is developed, it provides the nature of the exergy destruction and the best strategy to increase the efficiency of the cycle. The evaporator and turbine are presented as the most promising pieces of equipment to be developed in new future research due to their avoidable endogenous nature of exergy destruction.

1. Introduction

The oceans cover more than 70% of the surface of the planet earth, it represents a large surface area exposed to energy from the sun. Ocean energy has been suggested as a potential renewable source for attenuating the effect of global warming and supplying a significant portion of the electricity needs of the rapidly increasing world population [1]. The ever-growing need for sustainable, non-polluting electricity led to the development of a wide variety of technologies to harvest wave [2] and ocean thermal energy conversion. The Ocean Thermal Energy Conversion (OTEC) technology takes advantage of the thermal gradient produced between the surface (20–30 °C) and the temperature at a certain depth in the ocean (3–10 °C), where solar energy does not penetrate. One of the main proposals is to use a closed Rankine cycle, which takes advantage of the thermal gradient of the ocean to produce power from a sustainable and clean perspective.

The ocean thermal energy conversion is a system that consists of a thermodynamic cycle capable of producing useful electrical power given the temperature differential between the surface and a certain depth of the ocean. The concept of OTEC can be traced back to studies and design from the 1920s, but it was a long time later when pilot plants were put into operation, for example, Mitsui et al. [3] considered that the on-land type small capacity OTEC plant is feasible in the Republic of Nauru considering the gross power output of 100 kW, it's interesting that the system was started with freon-22 as working fluid, ammonia was discarded due to its toxic characteristics. Uehara et al. [4] suggest 14 feasible locations for the installation of an OTEC system in the Philippine islands, the study discusses the economic aspects, the resistance of the system to meteorological phenomena, and the stability of the necessary thermal difference over time to provide a useful life horizon of 100 years. Tseng et al. [5] applied the Sequential Quadratic Programming as an optimization method to select the best operating conditions to determine the feasibility of a 5 MW OTEC plant to be built at Ho-Ping, Taiwan. According to the authors, some of the most important variables to consider are the temperature differential between the surface and the depth of the ocean, and the volume flow of seawater through the evaporator and condenser, among others. Nihous

* Corresponding author.
E-mail address: dcolorado@uv.mx (D. Colorado-Garrido).

https://doi.org/10.1016/j.renene.2024.120018
Received 24 February 2023; Received in revised form 24 November 2023; Accepted 12 January 2024
Available online 13 January 2024

Nomenclature

ΔH	Pump head (m)
Ja	Jacob number
$OTEC$	Ocean Thermal Energy Conversion
P	Pressure (kPa)
RSS	Residual Sum of Squares
S	Salinity ($g\,kg^{-1}$)
T	Temperature (°C)
T_{cs}	Temperature of secondary flow in the condenser (°C)
T_{ws}	Temperature of secondary flow in the evaporator (°C)
ΔH_{cs}	Total pump head of cold seawater (m)
ΔH_{ws}	Total pump head of warm seawater (m)
ΔT	Temperature difference (K)
ΔT_c	Pinch temperature difference in the condenser (°C)
ΔT_e	Pinch temperature difference in the evaporator (°C)
$\dot{E}_D$	Exergy destruction (kW)
$\dot{E}_D^{EN,AV}$	Endogenous available part of exergy destruction (kW)
$\dot{E}_D^{EN,UN}$	Endogenous unavailable part of exergy destruction (kW)
$\dot{E}_D^{EX,AV}$	Exogenous available part of exergy destruction (kW)
$\dot{E}_D^{EX,UN}$	Exogenous unavailable part of exergy destruction (kW)
$\dot{E}x$	Exergy flow rate ($kJ\,s^{-1}$)
$\dot{Q}$	Heat transfer (kW)
$\dot{Q}_c$	Heat flow in the condenser (kW)
$\dot{Q}_e$	Heat flow in the evaporator (kW)
$\dot{W}$	Power (kW)
$\dot{W}_{cs}$	Cold seawater pumping power (kW)
$\dot{W}_{net}$	Net power out (kW)
$\dot{W}_{ws}$	Warm seawater pumping power (kW)
$\dot{m}$	Mass flow ($kg\,s^{-1}$)
$\dot{m}_{cs}$	Mass flow of seawater of condenser ($kg\,s^{-1}$)
$\dot{m}_{wf}$	Mass flow of working fluid ($kg\,s^{-1}$)
$\dot{m}_{ws}$	Mass flow of seawater of evaporator ($kg\,s^{-1}$)
$\overline{Cp}$	Heat capacity ($kg\,m^2\,s^{-2}\,K^{-1}$)
$\overline{Cp}_{cs}$	Heat capacity at the mean temperature of the cooling seawater ($kg\,m^2\,s^{-2}\,K^{-1}$)
$\overline{Cp}_{ws}$	Heat capacity at the mean temperature of the heating seawater ($kg\,m^2\,s^{-2}\,K^{-1}$)
g	Acceleration of gravity ($m\,s^{-2}$)
h	Enthalpy ($kJ\,kg^{-1}$)
s	Specific entropy ($kJ\,kg^{-1}\,K^{-1}$)

Greek symbols

χ^2	Chi-Square test
ϕ_{exp}	experimental values
ϕ_{sim}	values of thermodynamic model
η	Efficiency
κ	Ratio of pinch point temperature difference

Subscripts

c	condenser
con	condensation
cs	cold seawater
e	evaporator
eva	evaporation
i, o	thermodynamic state (inlet, outlet)
p	pinch point
wf	working fluid
ws	warm seawater

and Vega [6] presented for the first time the integration of a 100 MW OTEC-Hydrogen conceptualization; plant layouts, piping, and fittings, connections, as well as the compact alternative design concept are drawn and presented to show the feasibility of integration. In recent years, Hamedi et al. [7] mention the possibility of building a 5 MW plant in the sea of Oman, it is interesting to note the competitiveness that oceanic technology presents against other cases of renewable or non-renewable sources based on cost indicators for each kW produced. Recently, Monte Carlo simulation was used to vary the size of an OTEC plant in Indonesia, a net electrical output of 100 MW was considered with a 30% power loss as a constraint, and under tropical ocean conditions, small variations of temperature throughout the year and relatively calm sea waters [8].

To the best of the author's knowledge, in the literature, significant efforts have been made to model thermodynamically the Rankine cycles involved in ocean thermal energy conversion technology. Sun et al. [9] optimizes efficiency and net power produced in a closed Rankine cycle involved in OTEC technology, in which, ammonia, r134a, and other wet refrigerants are studied in the modeling. The authors mention that it is easy to show that $\dot{W}_{net}$ is a function of the mass flow of warm seawater, the seawater surface temperature, the evaporation and condensation temperatures of the working fluid, the heat capacity, and the product of the global coefficient of heat transfer and heat transfer area. The mass flows assumed by the authors range from 1000 to 7000 $\frac{kg}{s}$ of the feed flow to the evaporator, obtaining up to theoretical maximum power of 1.8 MW. Idrus et al. [10] propose an integration scheme for an energy flow from an oil/gas offshore main platform to increase the efficiency of an OTEC cycle called Geo-Ocean thermal energy conversion. The calculated efficiencies for the Geo-Ocean cycle are in a range of 3.84 to 4.65, and the efficiencies calculated for the Geo-Ocean cycle are in a range of 3.84 to 4.65 depending on the degrees of superheated temperature degree of the working fluid before entering the turbine. A theoretical model and optimization techniques are used to propose an OTEC cycle in the San Blas archipelago, Panama by Vera et al. [11], the proposal includes benefits in aquaculture, estimates of surface temperature (26.5–30 °C) and at a certain depth of the ocean (5–15 °C), pinch temperature difference, with the aim of producing power close to 0.1 MW. The authors mention that there is a relationship between the temperature at a certain depth of the ocean with the length of the pipe and the power of the cold water pump. Bernardoni et al. [12] offer a technical-economic evaluation of OTEC closed cycles to identify the main design parameters of the plant such as the difference in temperature of the cold and hot seawater or the difference in temperature of the pinch point of the evaporator and the condenser; in the study, the authors evaluate multiple working fluids such as ammonia, propane, r22, r1234ze, methanol, and others. Yang and Yeh [13] maximize the net power production and minimize the construction area of the heat exchangers based on the condensation and evaporation temperature for an Organic Rankine Cycle.

In the thermodynamic models described above, the following annotations can be made:

- the authors assume the calculation of seawater properties as pure water,

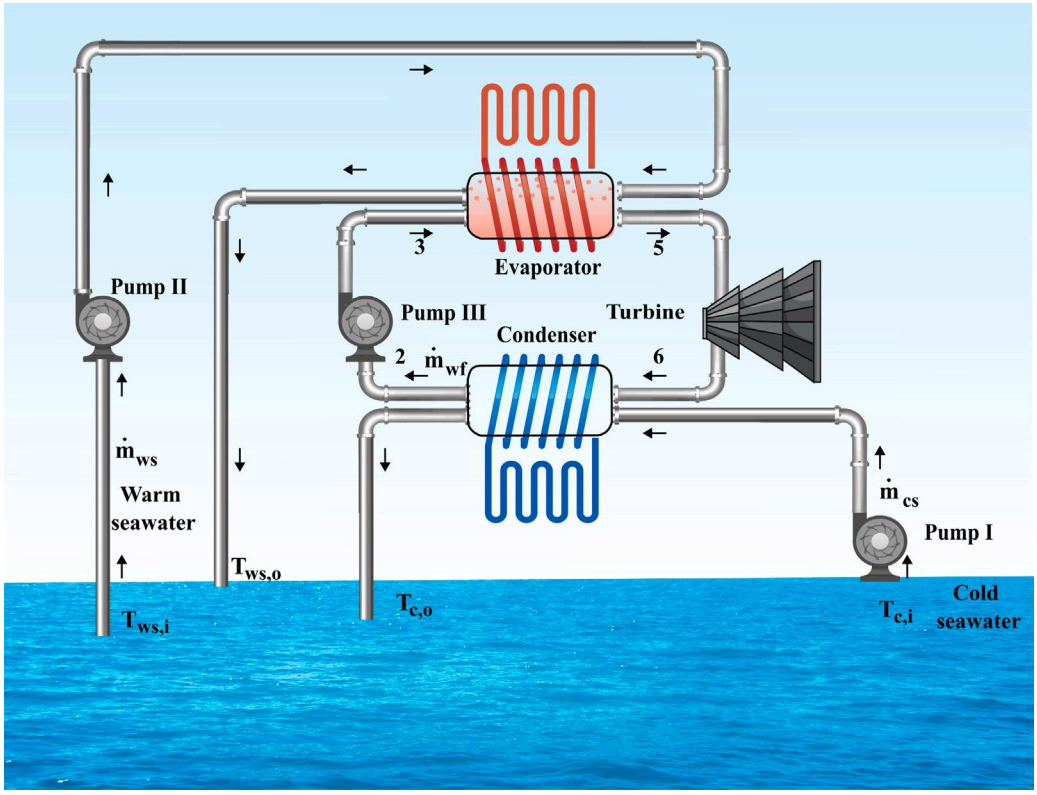

Fig. 1. Schematic diagram of the OTEC cycle.

- first, second law analysis of thermodynamics and techno-economic aspects are used,
- according to the slope of the saturation vapor curve in the temperature and entropy diagram, fluids can be classified as isentropic fluid, dry fluid, or wet fluid [14]. In the previously mentioned OTEC modeling systems, the preferred working fluid used is ammonia, due to its properties and net power obtained, and
- ammonia is a wet fluid and it is normally not suitable for the turbine in an Organic Rankine Cycle due to the formation of liquid droplets that tend to damage the blades.

Advanced exergy analysis was proposed by the research group led by Prof. George Tsatsaronis, such as [15], in which the exergy destruction of the system can be divided and consequently quantify the nature of each part. The method has been successfully applied to power cycles [16], Organic Rankine Cycles (ORC) [17,18], Kalina cycle for low temperature enhanced geothermal system [19] and it has been applied in renewable systems, such as geothermal [20] or solar energy [21]. To the best of the author's knowledge, it has not been applied in ocean thermal energy conversion technology.

According to Petrakopoulou et al. [22], the unavoidable (UN) designation for any kth component refers to exergy destruction that cannot be reduced, and can be imputed to two sources: the endogenous (EN) denomination which is attributed to inefficiencies in the heat and pressure transfer processes mainly, or defects in the manufacturing process, and the exogenous (EX) denomination which is referred to the effect of the exergy destruction of other components on the kth component evaluated. The avoidable (AV) term represents the real potential for improvement of the kth component evaluated, which can be reduced by applying technological efforts to increase its efficiency.

The hypotheses and methodology of the advanced exergy analysis consider that the exergy destruction of a system can be made up of four parts:

- The avoidable endogenous part $\dot{E}_{D,k}^{EN,AV}$,
- the avoidable exogenous part $\dot{E}_{D,k}^{EX,AV}$,
- the unavoidable endogenous part $\dot{E}_{D,k}^{EN,UN}$, and
- the unavoidable exogenous part $\dot{E}_{D,k}^{EX,UN}$.

Of the aforementioned, the following Eq. (1) must be satisfied:

$$\dot{E}_{D,k} = \dot{E}_{D,k}^{EN,AV} + \dot{E}_{D,k}^{EX,AV} + \dot{E}_{D,k}^{EN,UN} + \dot{E}_{D,k}^{EX,UN} \quad (1)$$

The following novelties of the present research are listed.

- The thermodynamic model is improved to evaluate an OTEC power cycle; in this research, the pinch difference temperature is added to the modeling of the condenser and evaporator to assess its impact on net power output and efficiency. The model has the versatility to use dry, wet or even isentropic working fluids.
- The model is compared with experimental data [23] satisfactorily.
- All the models that have been reported in the literature assume the calculation of enthalpy, entropy, and consecutively of exergy assuming pure water on the outside of the heat exchangers since this produces an imprecision in the calculations based on the second law of thermodynamics. In this investigation, appropriate correlations are used to calculate the thermo-physical properties of seawater according to [24].
- This research provides a thermodynamic study through an advanced exergy analysis of a closed Rankine cycle involves in ocean thermal energy conversion technology, which splits the exergy destruction into its endogenous or exogenous and avoidable or unavoidable parts in order to estimate a potential improvement and propose a better technological strategy to improve the system. A parametric study is presented to estimate the effect of the mass flow of warm seawater and the ocean bottom temperature at the condenser inlet on the exergy destruction of the system.

This work has been organized as follows: Section 2 illustrates an ocean thermal energy conversion power plant of our interest. Section 3

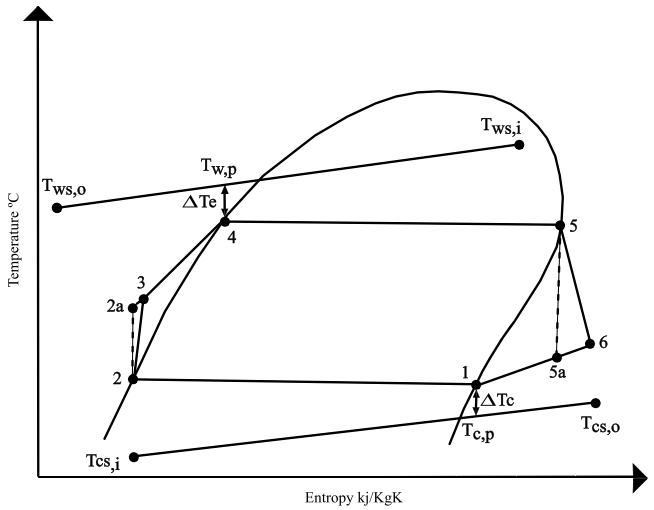

Fig. 2. Temperature against entropy diagram.

presents the entire methodology integrating different steps. Section 4 describes the main results and discussion of this work. Finally, the main conclusions are described.

2. System description

Fig. 1 shows the conceptual ocean thermal energy conversion power cycle under research. The main components of the cycle are an evaporator, a turbine, a condenser, a cold seawater pump (Pump I), a warm seawater pump (Pump II), and a working fluid pump (Pump III). According to this technology, the cycle was able to produce electrical power using a refrigerant as the working fluid [25], the cycle takes advantage of the temperature differential between the ocean surface and seawater at a certain depth. The working fluid leaving the condenser (2) is pumped to the evaporator at high pressure (3), the working fluid is evaporated by means of the heat source reaching its state of saturated vapor. The vapor leaving the evaporator (5) is expanded in the turbine (6) and it produce mechanical work and later electric power. Then, the mixture (steam and liquid) to a certain quality at lower pressure passes through the condenser reaching its state of saturated liquid (2), repeating the cycle. The seawater mass flow ($\dot{m}_{ws,i}$) at ocean surface temperature ($T_{ws,i}$) is pumped to be used as a heat source in the evaporator, the seawater from the ocean surface transfers energy to the working fluid and leaves the evaporator at a lower temperature ($T_{ws,o}$). On the other hand, seawater is pumped from a certain depth of the ocean ($\approx$ 1000 m) to be used as cooling water in the condenser ($T_{cs,i}$). In the condenser, the working fluid is condensed taking advantage of the heat transfer to the seawater, which obtains an increase in temperature ($T_{cw,o}$). The thermal gradient between the surface and the deep ocean seawater is defined as $T_{ws,i} - T_{cw,i}$. Fig. 2 shows the thermodynamic diagram, entropy against temperature, with corresponding states of entire cycle of this research.

3. The entire methodology, advanced exergy analysis

Taking into account the description of the system made in the previous section, the following methodology was followed: (i) the mass balances and the first law analysis of thermodynamics was carried out, (ii) the exergy balances are formulated for the entire system and each main component to quantify exergy destruction, and subsequently (iii) the advanced exergy analysis was implemented to determine the potential for system improvement.

The first law analysis of thermodynamics have been used to assess the performance of an ocean thermal energy conversion cycle. According to the characteristics of the ocean thermal energy conversion power cycle, the following assumptions are enlisted:

- Temperature (T), pressure (P), and salinity (S) are thermodynamically consistent and could be compared with experimental advances in ocean thermal technology.
- The system operates in steady-state conditions [26].
- The pieces of equipment that heat transfer are considered to be insulated [27].
- The pressure drop in the main components is neglected. The pressure drop due to the effect of friction in the transport of seawater by pumps I and II is neglected, due to the possibility of having storage tanks before entering the OTEC system. The power of the seawater pumps is considered for the calculation of the net power output of the entire cycle.
- The expansion process in the turbine is considered non-isentropic.
- Equilibrium and saturation conditions of the working fluid are assumed at the outlet of the condenser and evaporator.
- The pumps add work to the working fluid or seawater assuming them as a non-isentropic process [10].

The OTEC shown in Fig. 1, contains four main components: an evaporator, a condenser, a turbine, pump, and the thermodynamic performance can be described with the mass and energy balances.

The general mass balance is in agreement with:

$$\sum \dot{m}_{input} = \sum \dot{m}_{output} \tag{2}$$

The energy balance of each component is obtained by simplifying the first law of thermodynamics for each case:

$$\left(\sum \dot{m}_{input} h_{input} + \sum \dot{Q}_{input}\right) - \left(\sum \dot{m}_{output} h_{output} + \sum \dot{Q}_{output}\right) + \dot{W} = 0 \tag{3}$$

where $\dot{W}$ means power and appears in the energy balance of the turbine and pump, while $\dot{Q}$ is the heat flux and must be determined for the evaporator and condenser.

It is well known that the net power of the OTEC ($\dot{W}_{net\ OTEC}$) cycle is:

$$\dot{W}_{net\ OTEC} = \dot{W}_{net} - \dot{W}_{cs} - \dot{W}_{ws}, \tag{4}$$

where $\dot{W}_{ws}$ is the warm seawater pumping power, $\dot{W}_{cs}$ is the cold seawater pumping power and $\dot{W}_{net}$ is the net power out which is the difference between the turbine power ($\dot{W}_{turbine}$) and pump power ($\dot{W}_{pump}$), i.e., $\dot{W}_{net} = \dot{W}_{turbine} - \dot{W}_{pump}$.

In ocean thermal energy conversion technology, the pumping power of seawater at the surface and at certain depths influences the calculation of $\dot{W}_{net}$ and the selection of the appropriate T_{eva}. The cold seawater pumping power is calculated as:

$$\dot{W}_{cs} = \frac{\dot{m}_{cs} \Delta H_{cs} g}{\eta_{pump}}, \tag{5}$$

whereas the warm seawater pumping power is calculated as

$$\dot{W}_{ws} = \frac{\dot{m}_{ws} \Delta H_{ws} g}{\eta_{pump}} \tag{6}$$

where ΔH_{cs} and ΔH_{ws} are the total pump head of the cold and warm seawater piping respectively, η_{pump} denote the isentropic efficiency of the pumps, g is the acceleration of gravity, whereas, $\dot{m}_{ws}$ and $\dot{m}_{cs}$ are the mass flow of seawater at the secondary flow inlet of the evaporator and condenser, respectively.

Now, considering an energy balance for the system in a steady state it obtains that the change in the energy of the system in a given time interval is zero, moreover, the kinetic and potential energy terms are neglected, so the energy balance remains, that is, the sum of the powers equals the heat flows sum ($\sum \dot{W} = \sum \dot{Q}$). Consequently, the net power output was obtained by

$$\dot{W}_{net} = \dot{W}_{turbine} - \dot{W}_{pump} = \dot{Q}_e - \dot{Q}_c \tag{7}$$

with $\dot{Q}_e$ and $\dot{Q}_c$ denoting the heat fluxes in the evaporator and condenser, respectively.

On the other hand, let $T_{ws,i}$ and $T_{cs,i}$ be the inlet temperatures of secondary flow in the evaporator and condenser corresponding to the surface temperature and a certain depth of the ocean, whereas $\dot{m}_{ws,i}$ and $\dot{m}_{cs,i}$ are the mass flow of seawater at the secondary flow inlet of the evaporator and condenser. The pinch temperature difference in the evaporator (ΔT_e) and condenser (ΔT_c) are $\Delta T_e = T_{w,p} - T_{eva}$ and $\Delta T_c = T_{con} - T_{c,p}$. Moreover, $\overline{Cp}_{ws}$ and $\overline{Cp}_{cs}$ are the heat capacity calculated at the mean temperature of the heating and cooling seawater, respectively. The heat fluxes in the evaporator and condenser can be calculated by

$$\dot{Q}_e = \dot{m}_{ws,i}\overline{Cp}_{ws}\left(Ja_e + 1\right)\left(T_{ws,i} - T_{eva} - \Delta T_e\right) \tag{8}$$

$$\dot{Q}_c = \dot{m}_{cs,i}\overline{Cp}_{cs}\left(Ja_c + 1\right)\left(T_{con} - \Delta T_c - T_{cw,i}\right) \tag{9}$$

The Jacob number is defined as the ratio between sensible and latent heat taking as a reference for the secondary flow or working fluid. The Jacob number in the evaporator and condenser are denoted by Ja_e and Ja_c, and for the evaporator can be defined as follows:

$$Ja_e = \frac{T_{w,p} - T_{ws,o}}{T_{ws,i} - T_{w,p}} = \frac{h_4 - h_3}{h_5 - h_4} \tag{10}$$

Taking the Eq. (10) and the pinch temperature differential definitions, Ja_e can be expressed as follows:

$$Ja_e = \frac{T_{eva} + \Delta T_e - T_{ws,o}}{T_{ws,i} - T_{eva} - \Delta T_e} \tag{11}$$

For the condenser, the Jacob number can be expressed as follows:

$$Ja_c = \frac{T_{cs,o} - T_{c,p}}{T_{c,p} - T_{cs,i}} = \frac{h_6 - h_1}{h_1 - h_2} \tag{12}$$

Taking the Eq. (12) and the pinch temperature differential definitions, Ja_c can be expressed as follows:

$$Ja_c = \frac{T_{cs,o} - T_{con} + \Delta T_c}{T_{con} - \Delta T_c - T_{cs,i}} \tag{13}$$

The mass flow of the working fluid $\dot{m}_{wf}$ flowing in the Rankine cycle can be calculated with an energy balance in the evaporator according to:

$$\dot{m}_{wf} = \frac{\dot{m}_{ws}\overline{Cp}_{ws}\left(T_{ws,i} - T_{w,p}\right)}{h_5 - h_4} \tag{14}$$

At the same time, the energy balance in the condenser must be satisfied, according to the following balance:

$$\dot{m}_{wf} = \frac{\dot{m}_{cs}\overline{Cp}_{cs}\left(T_{c,p} - T_{cs,i}\right)}{h_1 - h_2} \tag{15}$$

The efficiency of the entire system is calculated according to:

$$\eta_{cycle} = \frac{\dot{W}_{net\ OTEC}}{\dot{Q}_e} \tag{16}$$

The ratio of the pinch point temperature difference between the evaporator and the condenser is defined by [28] and used in this work:

$$\kappa = \frac{\Delta T_e}{\Delta T_c} \tag{17}$$

The thermophysical properties, mass, energy balance equations, and the methodology described above were solved by means of a programming language. For the given $T_{ws,i}$, $T_{cs,i}$, $\dot{m}_{ws,i}$, $\dot{m}_{cs,i}$, pinch temperature difference in the evaporator ΔT_e and condenser ΔT_c, isentropic efficiency in the pump η_{pump}, and isentropic efficiency in the turbine $\eta_{turbine}$ the entire thermodynamic cycle can be calculated. Additionally, Algorithm 1 presents the sequence and logic followed in this research to create the thermodynamic model. This allows the model to be recreated in any programming language.

Algorithm 1 Iterative process to find $\dot{W}_{net\ OTEC}$ in eq. (4) and all thermodynamic points of the entire cycle

Require: Operating conditions: $\dot{m}_{ws,i}, \dot{m}_{cs,i}, T_{ws,i}, T_{cs,i}, \eta_{pump}, \eta_{turbine}$, $\Delta H_{w,pump}$, $\Delta H_{c,pump}$ and selection of working fluid.
Ensure: $\kappa = \frac{\Delta T_e}{\Delta T_c}$
for $\kappa = 0.8, 1.0, 1.2, ..., 3$ **do**
  for Steps = 1:1:2 **do**
    if Steps == 1 **then**
      $T_{eva} = [16 : 0.5 : 20]$;
    else if Steps ≠ 1 **then**
      $T_{eva} = T_{eva\ max}$
    end if
    for i = 1:1:length(T_{eva}) **do**
      solve $\dot{m}_{wf}$ for evaporator, eq. (14)
      first approximation $T_{con} = T_{eva} - \Delta T$
      C = 0;
      while C == 0 **do**
        solve $\dot{m}_{wf}$ for condenser, eq. (15)
        evaluate $e = \frac{\left|\dot{m}_{wf,e} - \dot{m}_{wf,c}\right|}{\dot{m}_{wf,e}}$
        if e ≥ 0.001 **then**
          $T_{con} = T_{con} - \Delta T$
          C = 0;
        else if e < 0.001 **then**
          C = 1;
          T_{con} calculated
        end if
      end while
    Calculate Ja_c in eq. (10), Ja_e in eq. (12), $T_{ws,o}$ and $T_{cs,o}$.
    Calculate $\dot{Q}_e$, $\dot{Q}_c$, $\dot{W}_{turbine}$ and $\dot{W}_{pump}$, $\dot{W}_{ws}$, $\dot{W}_{cs}$ and $\dot{W}_{net\ OTEC}$ using eq. (4).
    end for
    if Steps == 1 **then**
      Plot T_{eva} against $\dot{W}_{net\ OTEC}$ and **Find** $Max\ \left[\dot{W}_{net\ OTEC}\right]$
    end if
  $T_{eva\ max} = f\left(Max\ \left[\dot{W}_{net\ OTEC}\right]\right)$
  end for
end for

The second law analysis of thermodynamics is a powerful tool for determining the maximum work obtainable as a system interacts with a reference environment at an equilibrium state [29,30]. In accordance with [24] to carry out an appropriate assessment of systems involving seawater flow, it is necessary to use better approximations of thermo-physical properties and advanced methodologies. This is due to the large irreversible losses involved in seawater pumping systems. The analysis of the second law of thermodynamics is carried out with the following hypotheses:

- The nuclear, magnetic, chemistry, and electric terms were less appreciated.
- The kinetic and potential energy terms are considered negligible during the simplification of the global balances [29].
- Correlations for the calculation of thermo-physical properties of seawater such as enthalpy, entropy, and specific volume were taken by [30].

Exergy for a specific state in the cycle with reference to the dead state is defined as follows:

$$\dot{E}x = \dot{m}\left[\left(h - h_0\right) - T_0\left(s - s_0\right)\right] \tag{18}$$

where h is the enthalpy, s is the entropy of each system state, and the reference or dead state was set at $T_0 = 0$ °C, $P_0 = 101.325$ kPa, $h_0 = 399.4$ kJ kg^{-1} and $s_0 = 3.796$ kJ kg^{-1} K^{-1}.

Table 1
Second law equations for the ocean thermal energy conversion power cycle.

Pieces of equipment	Exergy balance equations
Evaporator	$\dot{E}_{D,e} = \left(\dot{E}x_3 + \dot{E}x_{ws,i}\right) - \left(\dot{E}x_5 + \dot{E}x_{ws,o}\right)$
Condenser	$\dot{E}_{D,c} = \left(\dot{E}x_6 + \dot{E}x_{cs,i}\right) - \left(\dot{E}x_2 + \dot{E}x_{cs,o}\right)$
Turbine	$\dot{E}_{D,turbine} = \dot{m}_{wf} T_0 \left(s_6 - s_5\right)$
Pump I	$\dot{E}_{D,pump} = \dot{m}_{wf} T_0 \left(s_3 - s_2\right)$

The exergy destruction equation was defined by:

$$E_{D,k} = \sum_j \left(1 - \frac{T_o}{T_j}\right) \dot{Q}_j + \left(\sum_i \dot{E}x_i\right)_{input} - \left(\sum_i \dot{E}x_o\right)_{output} - \dot{W} \quad (19)$$

The obtained second law equations for the main components of the ocean thermal energy conversion power cycle are given in Table 1.

The total exergy destruction of the entire system $\dot{E}_{D,total}$ is calculated as the sum of the irreversibility loss of each component, as follows:

$$\dot{E}_{D,total} = \sum \dot{E}_{D,k}; \sum \dot{E}_{D,k} = \dot{E}_{D,turbine} + \dot{E}_{D,e} + \dot{E}_{D,c} + \dot{E}_{D,pump} \quad (20)$$

Further, the system exergetic efficiency is defined as the ratio of the net work produced and the exergy that enters the system, it is calculated according to:

$$\eta_{II} = \frac{\dot{W}_{neto}}{\dot{m}_{wf}\left[\left(h_{ws,i} - h_{ws,o}\right) - T_0\left(s_{ws,i} - s_{ws,o}\right)\right]} \quad (21)$$

Advanced exergy analysis quantify each term of Eq. (1), the total exergy destruction within the kth component $\dot{E}_{D,k}$ must be calculated using the concepts and equations previously illustrated and titled the second law analysis of thermodynamics. $\dot{E}_{D,k}^{EN}$ refers to the endogenous part of $\dot{E}_{D,k}$ this means that the k-component operates with its actual efficiency, while the other components operate ideally. The exogenous part of the exergy destruction in the kth component is $\dot{E}_{D,k}^{EX}$ and is attributed to the irreversibilities that occur in the remaining components. The following equation must be satisfied:

$$\dot{E}_{D,k} = \dot{E}_{D,k}^{EN} + \dot{E}_{D,k}^{EX} \quad (22)$$

The unavoidable part of exergy destruction $\dot{E}_{D,k}^{UN}$ is attributable to technological limitations of the k-component, expressed in heat transfer losses and pressure drops, this cannot be reduced. The avoidable part of the exergy destruction $\dot{E}_{D,k}^{AV}$ results from the subtraction of the $\dot{E}_{D,k}^{UN}$ part of the exergy destruction of the k-component, this part represents the potential for improvement of the component. The following expression must hold:

$$\dot{E}_{D,k} = \dot{E}_{D,k}^{UN} + \dot{E}_{D,k}^{AV} \quad (23)$$

The combination of both divisions in Eqs. (22) and (23) takes us to the Eq. (1), and therefore advanced exergy analysis can be formulated as the following:

$$1 = \frac{\dot{E}_{D,k}^{EN,AV}}{\dot{E}_{D,k}} + \frac{\dot{E}_{D,k}^{EX,AV}}{\dot{E}_{D,k}} + \frac{\dot{E}_{D,k}^{EN,UN}}{\dot{E}_{D,k}} + \frac{\dot{E}_{D,k}^{EX,UN}}{\dot{E}_{D,k}} \quad (24)$$

Each of the terms of the Eq. (1) and (24) can be explained according to the following. The avoidable endogenous $\dot{E}_{D,k}^{EN,AV}$ part represents the potential for improvement of the component attributable to new designs that increase its efficiency. The avoidable exogenous $\dot{E}_{D,k}^{EX,AV}$ part represents the possible increase in system efficiency when a change in configuration is evaluated. The unavoidable endogenous $\dot{E}_{D,k}^{EN,UN}$ part is attributed to the technological or material limitations of the component, it cannot be reduced. The unavoidable exogenous $\dot{E}_{D,k}^{EX,UN}$ part is due to technological limitations in other components of the system and its influence on the evaluated component, this cannot be reduced.

The procedure and suggestions explained by [18,31] has been followed. First, a real cycle is defined and assumes that there is a large pinch temperature difference between the components that transfer heat. Then, to estimate the viability of the cycle, like many other authors, an ideal cycle was assumed, which has a minimum pinch temperature difference in the heat exchangers and no pressure drops, at the same time an isentropic hypothesis in the mechanical devices. Then, a third configuration was necessary, the unavoidable cycle, which considers a finite minimum pinch temperature difference.

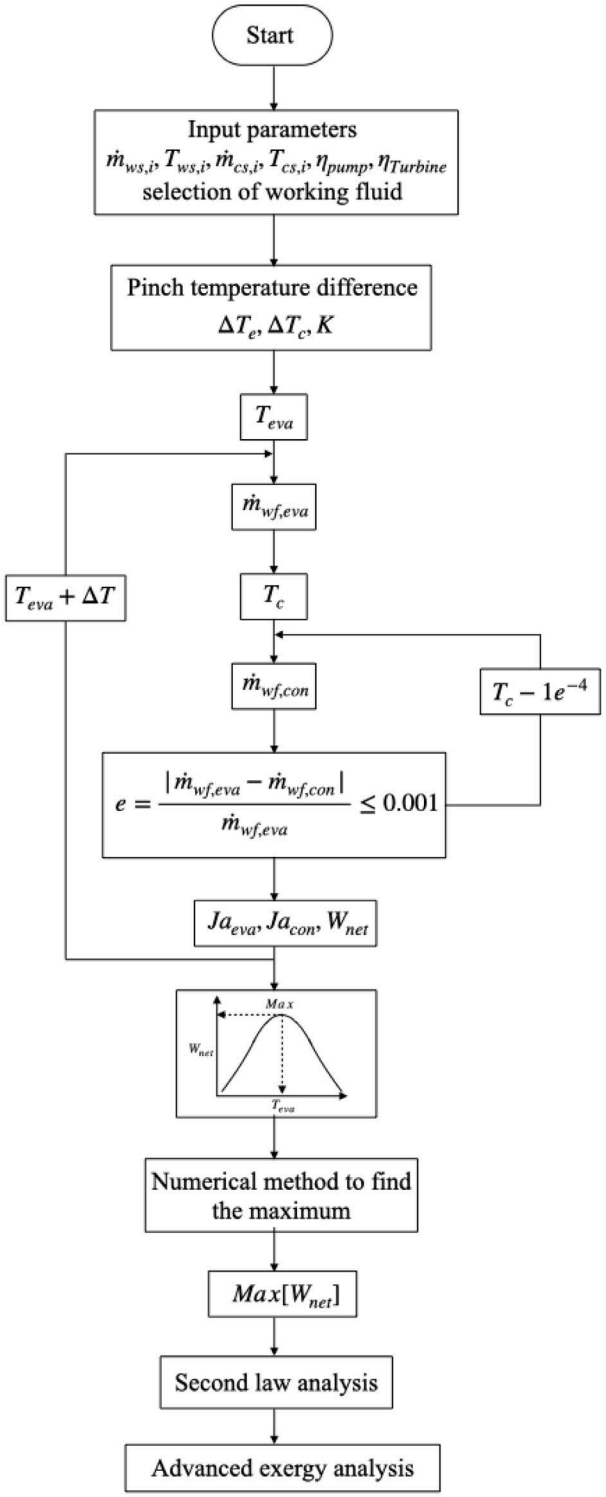

Fig. 3. The flowchart of calculation procedure.

Taking into account the above information, the steps suggested by [32] were followed:

- $\dot{E}_{D,k}$ for each component of the system is calculated,
- $\dot{E}_{D,k}^{UN}$ is calculated assuming unavoidable cycle settings and a finite minimum pinch temperature difference,
- the k-component (condenser, evaporator, turbine, or pump) to be evaluated is selected,
- The selected component is evaluated with a real temperature differential assuming the other components in ideal conditions, as a result $E_{D,k}^{EN}$ is obtained,
- the selected component was considered to have unavoidable settings and the other components were configured with ideal conditions. Thus, the unavoidable endogenous $E_{D,k}^{EN,UN}$ part of the exergy destruction was calculated.
- the following Eqs. (25), (26), (27) and (28) are solved to calculate the rest of the parts of the exergy destruction:

$$\dot{E}_{D,k}^{EN,AV} = \dot{E}_{D,k}^{EN} - \dot{E}_{D,k}^{EN,UN} \tag{25}$$

$$\dot{E}_{D,k}^{EX} = \dot{E}_{D,k} - \dot{E}_{D,k}^{EN} \tag{26}$$

$$\dot{E}_{D,k}^{EX,UN} = \dot{E}_{D,k}^{UN} - \dot{E}_{D,k}^{EN,UN} \tag{27}$$

$$\dot{E}_{D,k}^{EX,AV} = \dot{E}_{D,k}^{EX} - \dot{E}_{D,k}^{EX,UN} \tag{28}$$

This series of steps is repeated for each component taking into account the accuracy of the algorithm and the appropriate thermo physical properties.

Fig. 3 shows the flowchart of the *calculation procedure* for the ocean thermal energy conversion cycle under study. Once the convergence criteria have been satisfied $e \leq 0.001$, the system has been modeled and the results can be analyzed.

Remarks. A relevant aspect in the modeling of OTEC cycles is *the appropriate selection of the working fluid.* The designs and prototypes reported in the literature mention ammonia as the fluid that provides the best operating conditions for an ocean thermal conversion cycle. Given the shape of the saturation curve on the temperature vs. entropy diagram, ammonia is classified as a wet fluid. Otherwise, dry refrigerants such as r114, r123, r245ca, and r113 could be evaluated. The selection of this class of working fluids is based on avoiding erosion phenomena in the turbine blades, guaranteeing expansion in superheated steam conditions. Previous investigations have demonstrated the technical and economic feasibility of using dry refrigerants in power cycles, for example in the geothermal field [33]. Therefore the assessment of this class of dry refrigerants in the OTEC system is evaluated in the present research.

4. Results and discussion

This section presents the results corresponding to (i) the comparison of numerical against simulated results using ammonia as working fluid, (ii) results of the energy and conventional exergy analysis using dry refrigerants and finally (iii) the results and strategy for improving the cycle based on advanced exergy analysis and parametric analysis.

4.1. Experimental validation of the thermodynamic model

The thermodynamic modeling and simulation code were developed and it has been carefully verified, whenever possible, with experimental and numerical results obtained from a 15 kW ocean thermal energy conversion system of the Rankine cycle presented by Chen et al. [23].

The Fig. 4 shows a comparison between the thermal cycle efficiency calculated with the thermodynamic model presented in this research

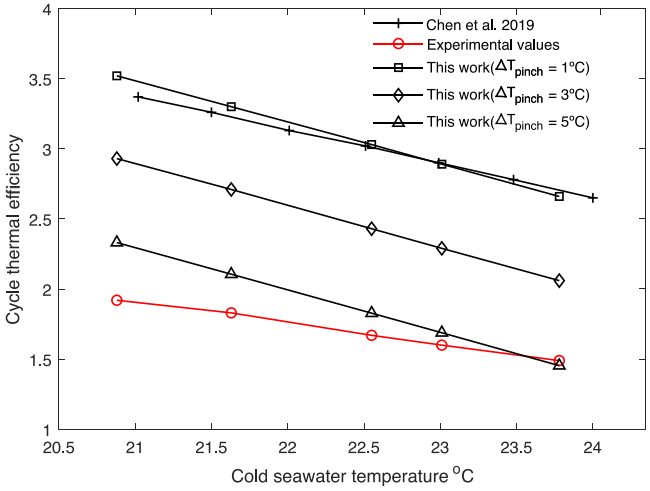

Fig. 4. Comparison of thermal cycle efficiency against cold seawater temperature of the present model, experimental results, and model by Chen et al. [23].

Table 2
Numerical results for illustrate the experimental development in [23].

Operation variable	value
$\dot{m}_{ws,i}$	46.7137 $\frac{kg}{s}$
$\dot{m}_{cs,i}$	93.4274 $\frac{kg}{s}$
$\dot{m}_{wf}$	0.4961 $\frac{kg}{s}$
T_{eva}	34.9801 °C
T_{con}	27.4635 °C
$T_{ws,i}$	40.8291 °C
$T_{ws,o}$	37.8889°C
$T_{cs,i}$	23.0000 °C
$T_{cs,o}$	24.4691 °C
Ja_{eva}	0.0320
Ja_{con}	0.0038

considering a ΔT_{pinch} = 1, 3 and 5 K, Chen's thermodynamic model, and experimental data [23] against the cold seawater temperature.

For the model presented in this paper, the following steps were followed:

1. As a first step, the thermodynamic model and algorithm 2 were used to find the mass flow of the warm stream of seawater corresponding to the required power.
2. The following operating and design conditions were assumed as inputs: the turbine inlet temperature was 42 °C and the pressure 1350 kPa, $\eta_{turbine} = 0.85$, $\eta_{pump} = 0.85$, $\Delta T_{pinch} = 3$ K, $\dot{W}_{req} = 15kW$, and ammonia is selected as the working fluid.
3. the following hypotheses were added $T_{ws,o} = T_{ws,i} + 3$ and $T_{w,p} = T_{eva} + \Delta T_{pinch}$.
4. The model calculates T_{con} based on T_{eva}, then calculates an error between $T_{ws,o}$ calculated and proposed, which must be less than 0.01 to obtain the result.
5. By an iterative process, the $T_{ws,o}$ and $T_{cs,o}$, Ja_{con} and Ja_{eva} were found. Then, changes in the available cold water temperature are made.
6. Finally, the thermal efficiency of the cycle is calculated.

Algorithm 2 shows the sequence to calculate the mass flow of warm seawater entering the evaporator to obtain the net power required.

The effect of the pinch temperature differential ΔT_{pinch} on the efficiency calculation is adequately illustrated. As can be seen in Fig. 4

Algorithm 2 Iterative process to find $\dot{m}_{ws,i}$ for 15 kW

Require: Operating conditions: $T_{cs,i}, T_5, P_4, \eta_{pump}, \eta_{turbine}, \Delta T_c = 3, \Delta T_e = 3, \dot{W}_{required} = 15kW$ and ammonia as working fluid.
for $\dot{m}_{ws,i} = 10 : 5 : 30$ **do**
$\dot{m}_{cs,i} = 2\dot{m}_{ws,i}$
First assumption $T^*_{ws,o} = T_{eva} + \Delta T$
D = 0;
while D == 0 **do**
$T_{ws,i} = T_{ws,o} + 3$
$T_{w,p} = T_{eva} + \Delta T_e$
Calculate $\dot{m}_{wf,e}$ using eq. (14)
C = 0;
while C == 0 **do**
$T_{c,p} = T_{cond} - \Delta T_c$
Calculate $\dot{m}_{wf,c}$ using eq. (15)
evaluate $e = \frac{|\dot{m}_{wf,e} - \dot{m}_{wf,c}|}{\dot{m}_{wf,e}}$
if e ≥ 0.001 **then**
$T_{con} = T_{con} - \Delta T$
C = 0;
else if e < 0.001 **then**
C = 1;
T_{con} calculated
end if
end while
Calculate Ja_c in eq. (10), Ja_e in eq. (12), $T_{ws,o}$ in eq. (11) and $T_{cs,o}$ in eq. (13).
Evaluate $e = \frac{|T_{cs,o} - T^*_{cs,o}|}{T_{cs,o}}$
if e > 0.01 **then**
$T^*_{cs,o} = T_{cs,o}$
D = 0;
else if e < 0.01 **then**
$T_{cs,o} = T_{cs,o}$
D = 1;
end if
end while
Calculate $\dot{Q}_e$ and $\dot{W}_{net} = \dot{W}_{turbine} - \dot{W}_{pump}$
end for
Plot $\dot{m}_{ws,i}$ against $\dot{W}_{net}$
Find $\dot{m}_{ws,i} = f\left(\dot{W}_{net} = \dot{W}_{required}\right)$

Table 3
Residual analysis between the simulated data and the experimental values of Chen et al. [23].

	ΔT_{pinch} = 1 °C	ΔT_{pinch} = 3 °C	ΔT_{pinch} = 5 °C	Chen et al. model
RSS	9.6035	3.1731	0.2818	8.4737
X_i	1.1408	0.3825	0.0359	1.0011

Table 4
Operation and design data considered for the thermodynamics and exergy analysis.

Operation Variables	
$T_{ws,i}$	28 °C [9]
$T_{cs,i}$	5 °C [9]
$\dot{m}_{ws,i}$	1000 $\frac{kg}{s}$ [9]
$\dot{m}_{cs,i}$	2 ×$\dot{m}_{ws,i}$ [35]
Salinity S	56 $\frac{gr}{l}$ [36]
Design considerations	
$\eta_{turbine}$	0.86 [10]
η_{pump}	0.85 [10]
ΔH_{ws}	2.62 m [10]
ΔH_{cs}	4.49 m [10]
ΔT_{pinch}	5 K [11]

Table 5
Thermodynamic data calculated for the ocean thermal energy conversion power cycle assuming κ = 1 and r123 as working fluid. Enthalpy and entropy in parentheses correspond to the pressure and temperature for pure water.

State	T (°C)	P (kPa)	$\dot{m}$ $\left(\frac{kg}{s}\right)$	h $\left(\frac{kJ}{kg}\right)$	s $\left(\frac{kJ}{kgK}\right)$	S $\left(\frac{g}{kg}\right)$
1	12.1833	55.3677	103.9029	388.7751	1.6625	–
2	12.1833	55.3677	103.9029	212.1577	1.0435	–
3	12.1905	71.8348	103.9029	212.1706	1.0435	–
4	18.6804	71.8348	103.9029	218.7131	1.0662	–
5	18.6804	71.8348	103.9029	392.6975	1.6624	–
6	12.9546	55.3677	103.9029	389.2937	1.6643	–
ws,i	28.0000	101.3250	1000	107.5370 (117.4624)	0.3416 (0.4091)	60
ws,o	23.5179	101.3250	1000	90.1847 (98.7226)	0.2834 (0.3464)	60
w,p	23.6804	101.3250	1000	90.8128	0.2855	60
cs,i	5.0000	101.3250	2000	19.0319 (21.1200)	0.0345 (0.0763)	60
cs, o	7.1897	101.3250	2000	27.3939 (30.3225)	0.0647 (0.1092)	60
c, p	7.1833	101.3250	2000	27.3694	0.0646	60

the present thermodynamic model assuming a ΔT_{pinch} = 3 K shows a similar trend to the experimental results, considering the cold seawater temperature from 21 to 24 °C. The numerical results presented by Chen et al. [23] overestimate the experimental results to a greater extent; this difference is assumed mainly to the consideration of T_{con} as a function of T_{eva}, which is not implicit in Chen's model. Some numerical results are shown in Table 2, it's the proposal that we assume operates in the experimental development. When the cold seawater temperature was 23 °C, the numerical thermal efficiency of the cycle was 2.05% and the experimental value was 1.356%. The absolute error of the thermal efficiency of the cycle is the absolute difference between the experimental value and the value that has been obtained in the simulation, for this work the absolute error was 0.694, while the absolute error of Chen at. al. model was 1.5524. The variation in the numerical and experimental results is due to the lack of information from the experimental equipment and its various system components.

In Fig. 4, for a $\Delta T_{pinch} = 1K$, the evaporation temperature increases and the condensation temperature decreases, which causes an increase in the cycle efficiency as they are directly related to the net output power, these numerical results are in agreement with Chen's results for an ideal model. It is interesting to note that, when ΔT_{pinch}= 5 K the model results are close to the experimental results of Chen et al. (2019).

A residual analysis is presented to evaluate the discrepancy between the experimental and simulated values with the thermodynamic model. The following tools were considered:

The residual sum of squares (RSS) is calculated using Eq. (29):

$$RSS = \sum_{i=1}^{n} \left(\phi_{sim} - \phi_{exp}\right)^2 \tag{29}$$

where ϕ_{sim} and ϕ_{exp} means the values obtained with the thermodynamic model and experimental values, respectively.

A non-parametric statistical analysis based on the absolute value of differences between experimental and simulated values, the sum of residuals, Chi-square X_i was used [34]:

$$X_i = \sum_{i=1}^{n} \frac{\left(\phi_{sim} - \phi_{exp}\right)^2}{\phi_{sim}} \tag{30}$$

Table 3 presents the results of the error analysis mentioned above. The analysis is carried out with ΔT_{pinch} = 1, 3 and 5 °C, it can be seen that when ΔT_{pinch} = 5 °C in the thermodynamic model, the results agree with the experimental results of Chen et al. [23].

Table 6
Numerical results of the analysis using the first and second law of thermodynamics assuming $\kappa = 1$.

Pieces of equipment	Heat load or power (kW)	Exergy destruction (kW)	Percentage of contribution of total exergy destruction (%)
Working fluid	**r114**		
Evaporator	18 902.99	272.0769	30.94
Condenser	18 550.07	551.4324	62.71
Turbine	219.04	55.2658	6.28
Rankine Cycle pump	3.82	0.5494	0.06
Warm sea water pump	30.23	–	
Cold sea water pump	103.63	–	
Total	–	879.3247	100%
Working fluid	**r123**		
Evaporator	18 757.26	269.7153	30.92
Condenser	18 404.94	547.0635	62.73
Turbine	353.6708	55.0464	6.31
Rankine Cycle pump	1.3453	0.1932	0.02
Warm sea water pump	30.2379	–	
Cold sea water pump	103.6398	–	
Total	–	872.0184	100%

Table 7
Efficiency parameters calculated for the ocean thermal energy conversion power cycle for several working fluids assuming $\kappa = 1$ and r123.

Efficiency	0.0116
System exergetic efficiency	1.4369

With the results shown in Fig. 4 and Table 3, it is clear that the ΔT_{pinch} in the evaporator and condenser affects the accuracy of prediction of the entire cycle efficiency.

4.2. Energy and exergy analysis results using dry refrigerants

The models, assumptions and features developed by Sun et al. [9], Mohd-Idrus et al. [10], Vera et al. [11], and Li et al. [37] were used to define the thermodynamic model to describe an ocean thermal energy conversion power plant simulated in this work, employing dry refrigerants.

The base case considering design and operation parameters constraints of the ocean thermal energy conversion power plant are described in Table 4. Table 5 displays the numerical results of temperature, salinity, mass flow, enthalpy, and entropy for the cycle using r123 as working fluid. It should be emphasized that, in Table 5, the results of enthalpy and entropy in the secondary flows of the evaporator and condenser from the ocean are calculated using appropriate correlations for seawater according to [24]; below each enthalpy and entropy result, the calculation considering pure water is shown (in brackets), clearly showing discrepancies in the calculation.

Energy and exergy numerical results of the ocean thermal energy conversion power cycle and its components are shown in Table 6; r114 and r123 working fluids were simulated in the Rankine cycle. As can be seen, the numerical results for heat flux and the contribution of each component to exergy destruction are very similar for r114 and r123 as working fluids. For r123 working fluid, the highest calculated power in the turbine of 353.67 kW was obtained, under these operating conditions, total exergy destruction of the cycle of 872.0184 kW was calculated. The condenser contributed more than 60% to the total exergy destruction. The evaporator showed the second highest contribution to the exergy destruction (up to 30%). Consequently, the turbine and pump were the most efficient pieces of equipment in the cycle. It was found that the percentage contributions per component to the total exergy destruction for r114 and r123 are very similar.

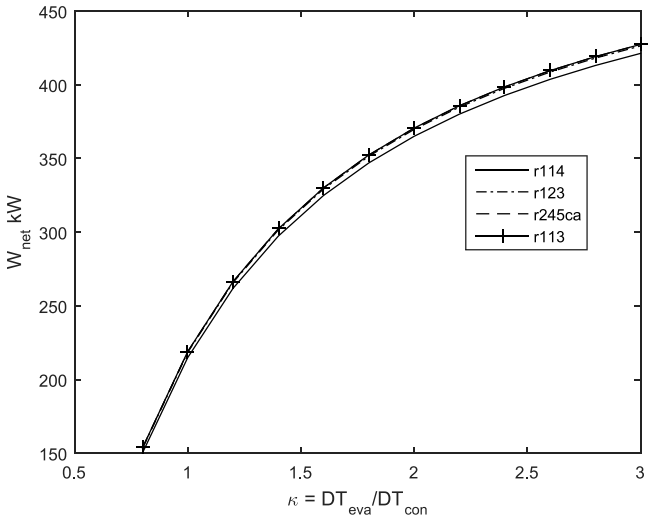

Fig. 5. Effect of pinch point temperature difference ratio (κ) on the net output power of the OTEC system for several dry refrigerants.

Table 7 displays the numerical results of exergy efficiency according to Eq. (21). It was calculated based on initial settings in Table 4 for r123.

Fig. 5 shows the numerical results of the OTEC net power calculated with Eq. (4). As can be seen, the net power of the cycle increases as κ increases, a similar behavior is observed in the work of [28]. The results are very similar between the simulated working fluids, this is because the OTEC cycle is designed and bounded by the surface temperature and at a certain depth of the ocean, which puts it at the bottom of the temperature vs entropy diagram. The turbine operates in superheated steam conditions, avoiding erosion problems in its design.

The use of second law analysis in processes depends to a large extent on the appropriate calculation of enthalpy and entropy for the working fluids, in our case where seawater is involved. In thermal systems, differences can be observed between the theoretical calculation considering pure water or seawater. Therefore, the estimation of the total exergy destruction depends on appropriate thermo-physical correlations. The total exergy destruction of the system was calculated while κ was increased in Fig. 6. As can be seen, the results assuming the thermophysical properties of pure water differ from the results using suitable correlations for seawater [24]. These discrepancies coincide

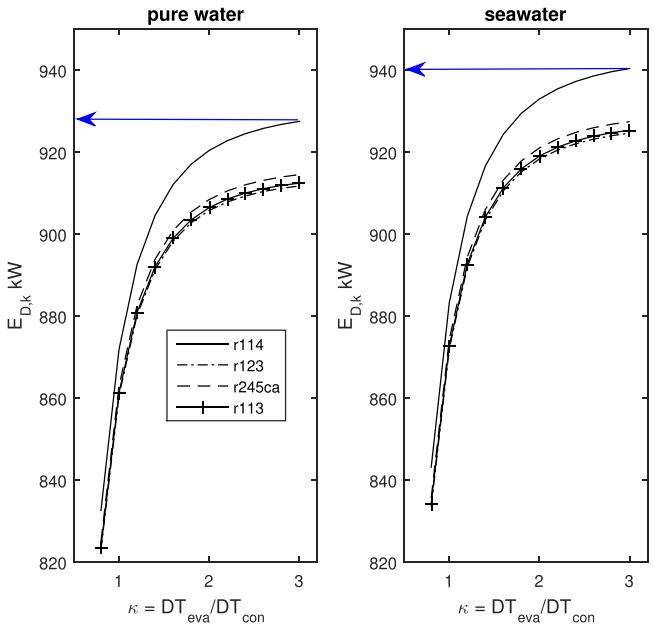

Fig. 6. Comparison between total energy destruction versus κ assuming the calculation of thermo-physical properties of pure water and seawater.

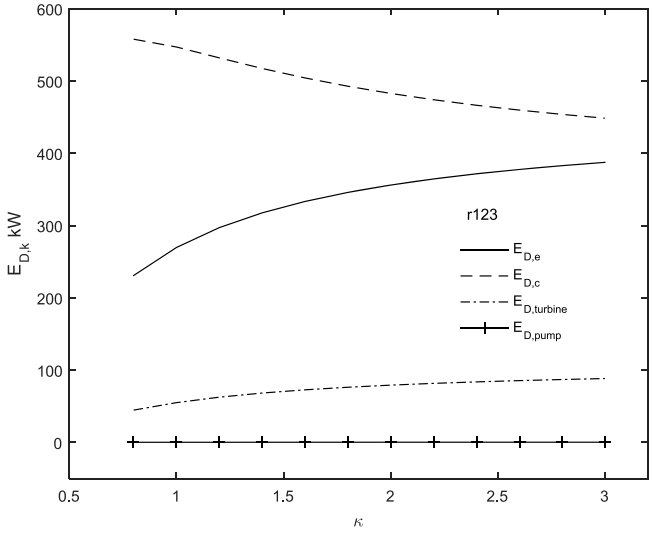

Fig. 7. Contribution of each component to the total exergy destruction against κ.

Table 8
Real, ideal, and unavoidable cycle settings.

Real cycle	Unavoidable cycle	Ideal cycle
ΔT_e = 3 K	ΔT_e = 1 K	ΔT_e = 0.5 K
ΔT_c = 3 K	ΔT_c = 1 K	ΔT_c = 0.5 K
$\eta_{turbine}$ = 0.85	$\eta_{turbine}$ = 0.95	$\eta_{turbine}$ = 1
η_{pump} = 0.7	η_{pump} = 0.9	η_{pump} = 1

with those presented and discussed by [38]. As an example, the difference in total exergy destruction at κ = 3 for r114 is illustrated in Figure Fig. 6. This difference is calculated for the entire range of k and all refrigerants, and for our research up to 12.25 kW difference in the calculation. The r123 and r114 are the working fluids that presented the lowest and highest value of exergy destruction respectively while κ was increased.

Fig. 7 shows the exergy destruction for each component as a function of the κ. The highest exergy destruction was calculated in the

Table 9
Numerical results of the ocean thermal energy conversion power cycle using r123.

	Total exergy destruction	Unavoidable	Avoidable
Entire cycle	937.9838	791.0342	146.9496
	100%	84.33%	15.66%

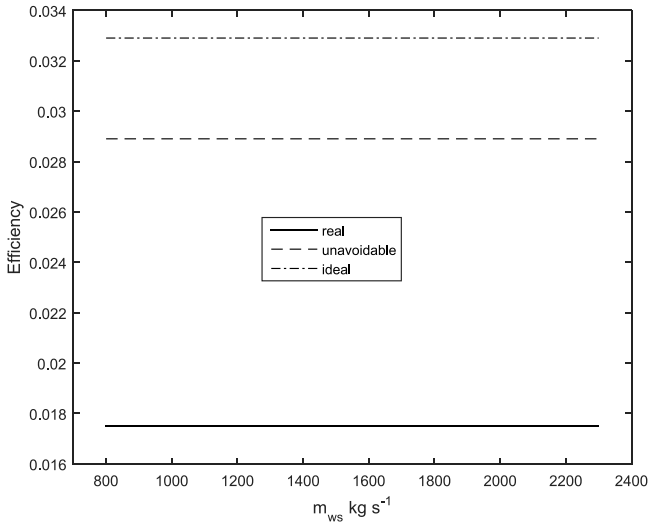

Fig. 8. Efficiency of entire cycle for ideal, unavoidable and real cycle configurations against warm mass flow in the evaporator.

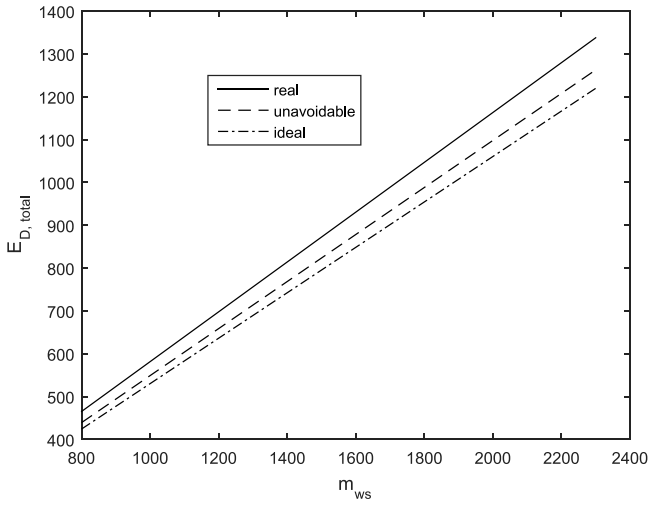

Fig. 9. Total exergy destruction against warm mass flow in the evaporator.

condenser, followed by the evaporator, turbine, and finally, the pump in the Rankine cycle, these pieces of equipment order are consistent with the numerical results presented by [12]. As can be seen, the condenser is the component that contributes the most to the total irreversibility of the entire system. Given the Eq. (17), it can be said that $\Delta T_c = \frac{\Delta T_e}{\kappa}$, this means that if κ values were increased in the range from 0.8 to 3, it is a consequence of a more efficient condenser in the heat transfer process and it was demonstrated that the irreversibility of the condenser decreased from 557.8639 kW to 448.5564 kW. Consequently, the irreversibility of the evaporator was increased from 230.9408 kW to 387.4613 kW because the ΔT_e moves away from an ideal value and decreases the heat transfer, assuming a value of κ = 1, the following relation was inferred: $\dot{E}_{D,e} = 0.5160\dot{E}_{D,c}$. These numerical results clearly indicate that to decrease the irreversibility of the OTEC system, proper design in the condenser and evaporator is

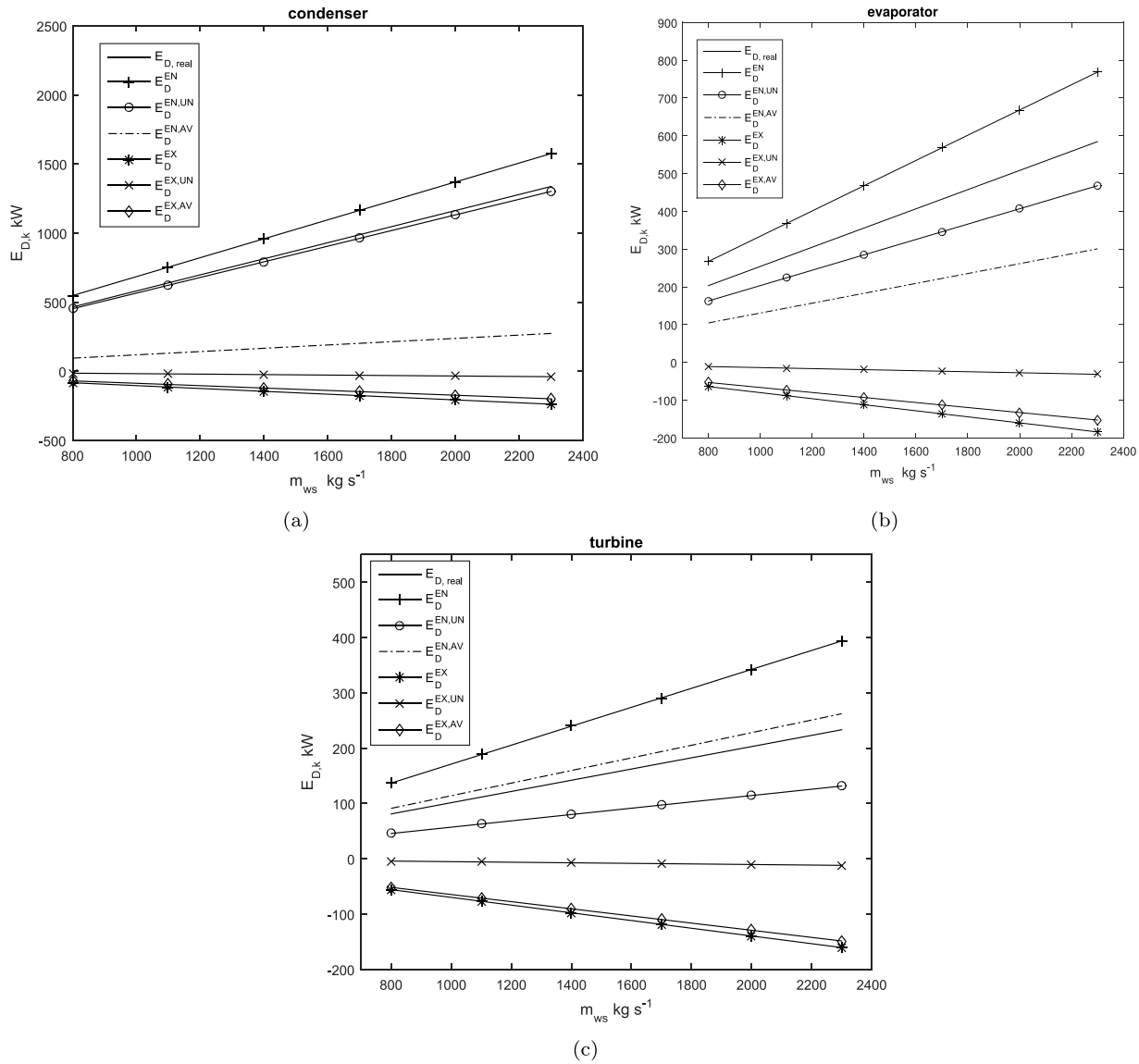

Fig. 10. Condenser, evaporator and turbine exergy destruction against warm mass flow in the evaporator.

essential. Regarding the other pieces of equipment, the turbine shows an increase in irreversibility from 44.6916 kW to 88.3520 kW, because the increase in the ΔT_e causes a decrease in the evaporation pressure and decreases the work produced in the turbine. It is interesting to note that the greatest increase in irreversibility of the turbine occurs for values of k from 0.8 to 2, after which it practically remains constant. The pump is the device that allows adding mechanical work to the working fluid and bringing it to a high-pressure level. The irreversibility of the pump is practically less than 0.2836 kW and remains practically constant for any κ value. Given the negligible contribution to the total irreversibility of the system, the pump is not considered an important piece of equipment, so its only timely maintenance is recommended.

4.3. Advanced exergy analysis results

Table 8 shows the settings for the real, ideal and unavoidable cycles following the suggestions of [31], and it represents technological limitations in the components of the analyzed cycle.

Table 9 presents the numerical results of the advanced exergy analysis methodology. As can be seen, a $\approx 15.66\%$ of the total irreversibility is of the avoidable type; it can be reduced and represents the potential for improvement of the entire system. A $\approx 84.33\%$ of the total irreversibility cannot be reduced. In this way, observing the results of the exergy analysis, the condenser is a component that contributes a significant percentage to the total destruction $\approx 62.73\%$ of the cycle, which can lead us to propose a strategy for technological improvement to the system, however, the splitting of the exergy destruction will lead us to discuss better ways.

A parametric analysis was developed in order to understand the nature of exergy destruction. Each term of the Eq. (1) was quantified following the advanced exergy methodology, as a function of the mass flow of warm seawater in agreement with [9] analysis and the ocean bottom temperature due to the importance in calculating tube length and pump design [11].

4.3.1. Effect of mass flow of warm seawater

Fig. 8 shows the numerical results of the efficiency under three different configurations: real (η_{real}), unavoidable $(\eta_{unavoidable})$, ideal (η_{ideal}). The highest values are those of the (η_{ideal}), followed by those of the $(\eta_{unavoidable})$; both are linear and remains constant when the mass flow of warm seawater increased from 800 $\frac{kg}{s}$ to 2300 $\frac{kg}{s}$. (η_{real}) was calculated in 0.0175. The numerical results shown in Fig. 8 agree with the results reported by Vera et al. [11] who performed a numerical simulation in which the warm mass flow in the evaporator increased

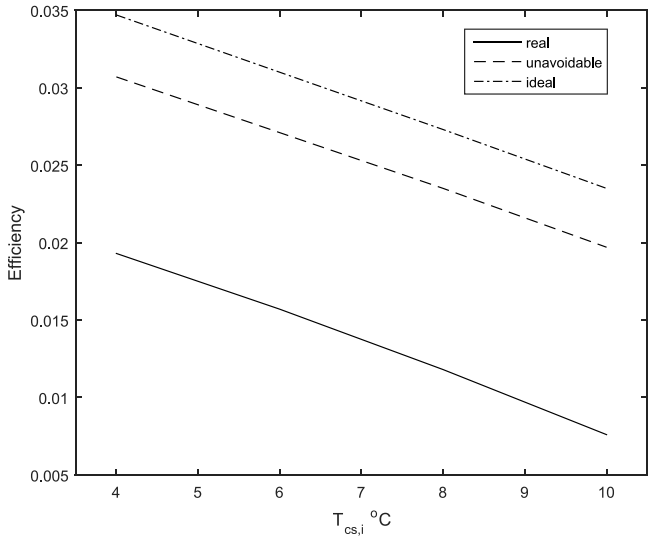

Fig. 11. Efficiency of the entire cycle for ideal, unavoidable, and real cycle configurations against ocean bottom temperature at condenser inlet.

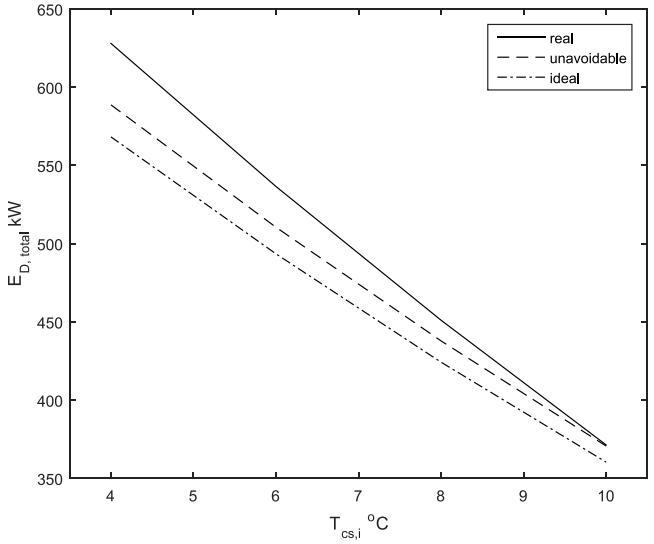

Fig. 12. Total exergy destruction against ocean bottom temperature at condenser inlet.

up to 2020 $\frac{kg}{s}$ assuming a hydraulic pipe diameter of 1 m and water pipe velocity of 2.5 $\frac{m}{s}$.

Total exergy destruction as a function of mass flow of warm seawater, as shown in Fig. 9; irreversibility for all three configurations increased by increasing the mass flow of warm seawater from 800 to 2300 $\frac{kg}{s}$. The real total exergy destruction increased from 465.2 kW to 1337.6 kW when the mass flux was increased in the range shown. Similar behavior of total exergy destruction for the ideal, avoidable and real settings were observed.

To carry out a detailed analysis of the main components that contribute to the exergy destruction of the system, the numerical results of the application of advanced exergy analysis in the condenser, evaporator, and turbine are shown in Fig. 10(a), (b) and (c) respectively. As can be seen, Fig. 10(a) presents the exergy destruction of the condenser while the mass flow of warm seawater was increased. The nature of the exergy destruction is completely endogenous and in a large percentage unavoidable (≈ 82.60%), while ≈ 17.4% of the endogenous exergy destruction can be reduced by implementing improvements in design or technology. This implies that making efforts in the design of the condenser to increase its efficiency will not positively benefit the entire system. It is interesting to note that the values of the exogenous part are negative, so increases in the efficiency of nearby components will not favor the efficiency of the condenser. The Fig. 10(b) presents the increase in the irreversibility of the evaporator as the mass flow of warm seawater increases, such that ≈ 60.87% of the exergy destruction was endogenous unavoidable and ≈ 39.13% was endogenous avoidable, which can mean an effective strategy to implement a better evaporator design to increase its efficiency. Decisions or strategies that increase heat transfer in the evaporator, for example, passive improvements or integration with solar technology, are recommended. Interesting are the results of the analysis for the turbine since ≈ 66.61% was endogenous avoidable, this means an area of opportunity in the investigation of this class of expansion devices in ocean technology energy conversion. The exogenous part of the exergy destruction is calculated as less than zero for the condenser, evaporator, and turbine, this means that an increase in the mass flux of warm seawater or a pinch temperature differential temperature in the other components does not affect the performance of these kinds of pieces of equipment.

4.3.2. *Effect of ocean bottom temperature at condenser inlet*

The ocean bottom temperature at the condenser inlet is another important operation variable to consider. In the ocean thermal energy conversion cycle, the temperature at which water enters the ocean bottom is related to the length of the tube, according to [11] a change of 4 °C to 8 °C can mean a change in tube length of up to 700 m. For economic studies as [10], the ocean bottom temperature and pipe length influence the cost of pumps included in the cost of purchased equipment. The effect of ocean bottom temperature at the condenser inlet on the exergy destruction using advanced exergy analysis is discussed below:

Fig. 11 shows the efficiency for the ocean thermal energy conversion cycle as a function of ocean bottom temperature at the condenser inlet, assuming the ideal, unavoidable and real configurations described previously. It was observed that all η decreased when the temperature increased, this corresponds to the increase in the condensation temperature of the cycle and the decrease in the net power produced in the expansion. The efficiency of all cycles presented a similar tendency, all of them decreased approximately by 60% when the ocean bottom temperature was raised from 4 °C to 10 °C. The effect of the ocean bottom temperature on the total exergy destruction is plotted in Fig. 12. Where it can be observed that the total exergy destruction decreases significantly as the ocean bottom temperature increases. As expected, the largest total exergy destruction values are for the real cycle, followed by the unavoidable cycle, and finally the cycle with ideal settings.

With respect to the condenser, evaporator, and turbine, Fig. 13 shows the numerical results of the exergy destruction splitting when the ocean bottom temperature was increased. Fig. 13(a) shows that the improvement potential $\dot{E}_D^{EN,AV}$ of the condenser remains practically constant in the study interval. The improvement potential of the condenser is not a function of the availability of cold water between 4 or 10 °C. The exergy destruction in the condenser $\dot{E}_{condenser}$ is produced by the decrease in the term $\dot{E}_D^{EN,UN}$, this means that if the cold water available is close to 4 °C, so its irreversibility is inevitable and unlikely to improve performance. The pinch temperature differentials of other pieces of equipment of the system do not have a favorable influence on the reduction of $\dot{E}_{condenser}$. It is interesting to note that the evaporator (see Fig. 13(b)) presents a similar behavior in the distribution of exergy to the condenser. In the evaporator, the improvement potential $\dot{E}_D^{EN,AV}$ does not depend on the ocean bottom temperature to which the working fluid is cooled in the condenser. Therefore, improvement strategies in the evaporator should not depend on the availability of cold water in the condenser, promoting the integration of the evaporator with other renewable technologies. The nature of the irreversibility of the turbine was displayed in Fig. 13(c). The exergy destruction decreased when the ocean bottom temperature

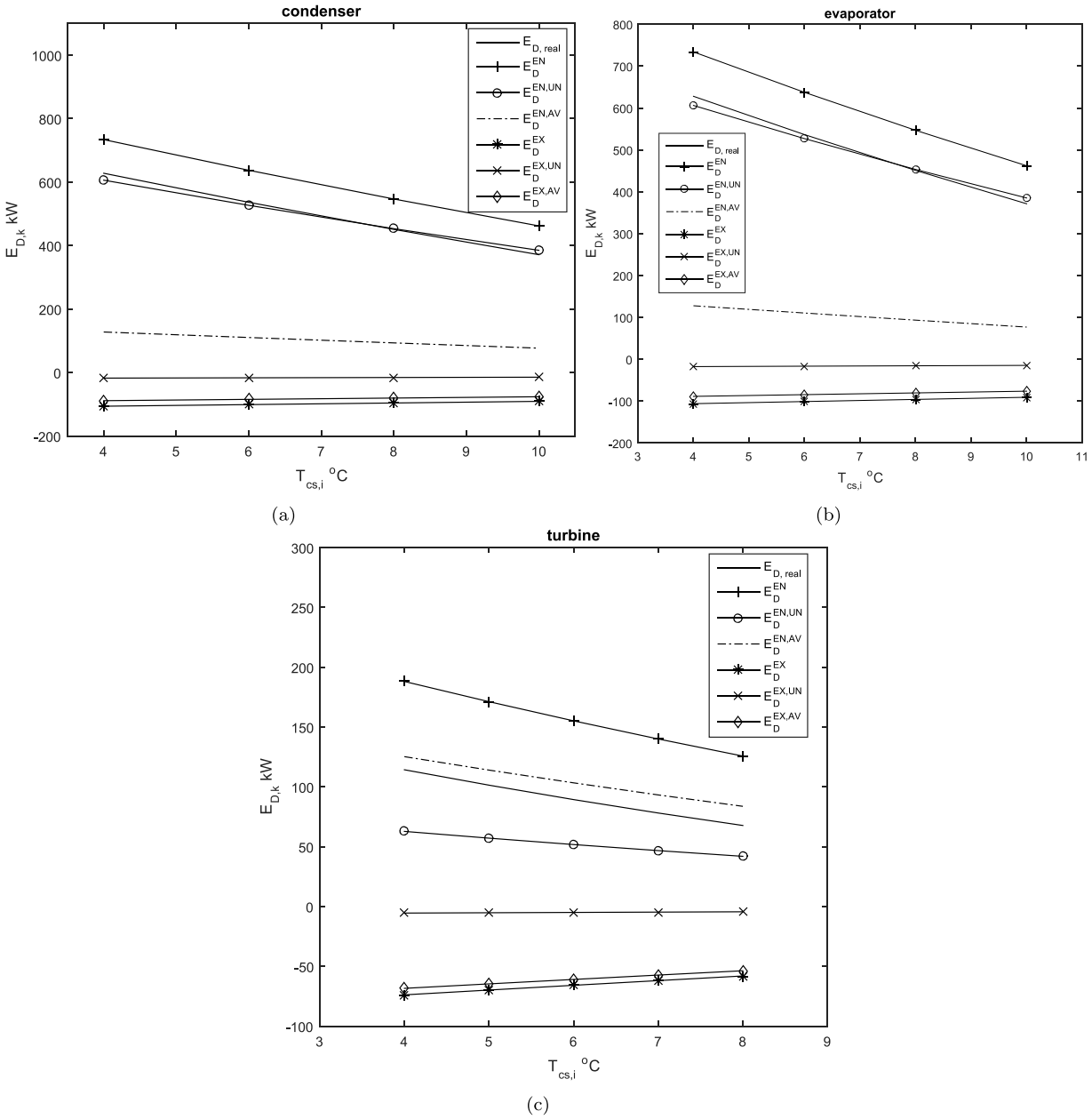

Fig. 13. Condenser, evaporator, and turbine exergy destruction against ocean bottom temperature at condenser inlet.

increased. The term avoidable is greater than the term unavoidable for the endogenous terms $\dot{E}_D^{EN,AV} > \dot{E}_D^{EN,UN}$, Therefore, it is advisable to increase the efficiency in the expansion to take advantage of this aspect. This means that the technological development of turbines considering a cold ocean water temperature close to 4 C is widely recommended. The exogenous part of the exergy destruction for the turbine is less than zero, so the efficiency of the rest of the components does not favorably influence the exergy destruction of the turbine.

5. Conclusions

The thermodynamic study was successfully developed in the research for an ocean thermal engineering conversion system. The main contributions of the present study are the following:

- The thermodynamic model developed in this research with $T_{ws,i}$ = 40.82 °C and $T_{cs,i}$ = 23 °C, $\Delta T_{pinch} = 3K$ calculates an efficiency to 2.05%. The numerical results of the present model against experimental and numerical results reported in the literature show the effect of the pinch temperature differential on the efficiency, showing results with an absolute error of less than 1.5% for a ΔT_{pinch} = 3 K. For dry refrigerants such as r114, r123, r245ca, and r113, the net power output calculated considering pinch temperature differential variations is insignificant, due to ocean temperature conditions, the discrepancies between fluids were found with the analysis of the second law of thermodynamics.
- Discrepancies of up to 12.25 kW were obtained by the use of appropriate correlations to calculate the enthalpy and entropy of seawater in the total exergy destruction results of the OTEC system compared to the assumption of pure water. According to the conventional exergy analysis, the condenser is the component that contributes the most to the irreversibility of the entire system (> 60%), followed by the evaporator (≈ 30%), turbine (≈ 6%), and finally the working fluid pump (< 1%).

- The potential for improvement of the OTEC system was quantified; for the studied base-case using r123 as working fluid, the total irreversibility of the system is 937.98 kW, from which 146.9496 kW are avoidable and represents 15.66% that could be reduced. The proposed strategy to increase the efficiency of the cycle is the following. First, the best area of opportunity for system improvement is found in the evaporator because it has a considerable amount of endogenous avoidable exergy destruction up to 40%. Integration strategies of the OTEC system with renewable energy (such as solar or geothermal) at points before, on, or after the evaporator seem to be the best options. Second, the turbine is the expansion device that owns $\dot{E}_D^{EN,AV} > \dot{E}_D^{EN,UN}$, this gives us opportunities for technological improvement, added to the benefits of using dry coolants that prevent erosion in blades. Finally, the exergy destruction of the condenser is endogenous unavoidable nature up to 80%, therefore putting effort into design or new technologies will not favorably increase the efficiency of the equipment.

CRediT authorship contribution statement

Dario Colorado-Garrido: Conceptualization, Methodology, Formal analysis, Writing – original draft, Project administration. **Emmanuel Mendoza-Bernal:** Validation, Investigation, Software. **Lili M. Toledo-Paz:** Investigation, Software, Visualization. **Beatris A. Escobedo-Trujillo:** Formal analysis, Investigation, Writing – original draft.

Declaration of competing interest

The authors declare that they have no known competing financial interests or personal relationships that could have appeared to influence the work reported in this paper.

Acknowledgments

We thank the anonymous reviewers and the editor-in-chief for his valuable stewardship of an earlier version of this manuscript. The second and third authors (Emmanuel Mendoza-Bernal and Lili M. Toledo-Paz) expresses his/her gratitude to CONAHCyT, Mexico for the scholarship awarded for postgraduate Master of Science studies. The first and fourth authors (Dario Colorado-Garrido and Beatris Escobedo-Trujillo) also thank CONAHCyT, Mexico for the financial support through the SNI for the research.

References

[1] Ayrton Alfonso Medina Rodríguez, Rodolfo Silva Casarín, Jesús María Blanco Ilzarbe, The influence of oblique waves on the hydrodynamic efficiency of an onshore OWC wave energy converter, Renew. Energy 183 (2022) 687–707, http://dx.doi.org/10.1016/j.renene.2021.11.061.

[2] K. Rezanejad, C. Guedes Soares, I. López, R. Carballo, Experimental and numerical investigation of the hydrodynamic performance of an oscillating water column wave energy converter, Renew. Energy 106 (2017) 1–16, http://dx.doi.org/10.1016/j.renene.2017.01.003.

[3] T. Mitsui, F. Ito, Y. Seya, Y. Nakamoto, Outline of the 100 kw OTEC pilot plant in the republic of mauru, IEEE Trans. Power Appar. Syst. PAS-102 (1983) 3167–3171, http://dx.doi.org/10.1109/TPAS.1983.318124.

[4] H. Uehara, C.O. Dilao, T. Nakaoka, Conceptual design of ocean thermal energy conversion (OTEC) power plants in the Philippines, Sol. Energy 41 (1988) 431–441, http://dx.doi.org/10.1016/0038-092X(88)90017-5.

[5] C.H. Tseng, K.Y. Kao, J.C. Yang, Optimal design of a pilot OTEC power plant in Taiwan, J. Energy Resour. Technol. 113 (1991) 294–299, http://dx.doi.org/10.1115/1.2905914.

[6] G.C. Nihous, L.A. Vega, Design of a 100 MW OTEC-hydrogen plantship, Mar. Struct. 6 (1996) 207–221, http://dx.doi.org/10.1016/0951-8339(93)90020-4.

[7] A.S. Hamedi, S. Sadeghzadeh, Conceptual design of a 5MWOTEC power plant in the Oman Sea, J. Mar. Eng. Technol. 16 (2017) 94–102, http://dx.doi.org/10.1080/20464177.2017.1320839.

[8] R. Adiputra, T. Utsunomiya, J. Koto, T. Yasunaga, Y. Ikegami, Preliminary design of a 100 MW-net ocean thermal energy conversion (OTEC) power plant study case: Mentawai island, Indonesia, J. Mar. Sci. Technol. 25 (2020) 48–68, http://dx.doi.org/10.1007/s00773-019-00630-7.

[9] F. Sun, Y. Ikegami, B. Jia, H. Arima, Optimization design and exergy analysis of organic rankine cycle in ocean thermal energy conversion, Appl. Ocean Res. 35 (2012) 38–46, http://dx.doi.org/10.1016/j.apor.2011.12.006.

[10] N.H. Mohd Idrus, M.N. Musa, W.J. Yahya, A.M. Ithnin, Geo-ocean thermal energy conversion (GeOTEC) power cycle/plant, Renew. Energy 111 (2017) 372–380, http://dx.doi.org/10.1016/j.renene.2017.03.086.

[11] D. Vera, A. Baccioli, F. Jurado, U. Desideri, Modeling and optimization of an ocean thermal energy conversion system for remote islands electrification, Renew. Energy 162 (2020) 1399–1414, http://dx.doi.org/10.1016/j.renene.2020.07.074.

[12] C. Bernardoni, M. Binotti, A. Giostri, Techno-economic analysis of closed OTEC cycles for power generation, Renew. Energy 132 (2019) 1018–1033, http://dx.doi.org/10.1016/j.renene.2018.08.007.

[13] M.H. Yang, R.H. Yeh, Analysis of optimization in an OTEC plant using organic Rankine cycle, Renew. Energy 68 (2014) 25–34, http://dx.doi.org/10.1016/j.renene.2014.01.029.

[14] C.R. Kuo, S.W Hsu, K.H. Chang, C.C. Wang, Analysis of a 50 kw organic Rankine cycle system, Energy 36 (2011) 5877–5885, http://dx.doi.org/10.1016/j.energy.2011.08.035.

[15] T. Morosuk, T. Tsatsaronis, Advanced exergy-based methods used to understand and improve energy-conversion systems, Energy 169 (2019) 238–246, http://dx.doi.org/10.1016/j.energy.2018.11.123.

[16] S. Tesch, T. Morosuk, G. Tsatsaronis, Advanced exergy analysis applied to the process of regasification of LNG (liquefied natural gas) integrated into an air separation process, Energy 117 (2016) 550–561, http://dx.doi.org/10.1016/j.energy.2016.04.031.

[17] J. Galindo, S. Ruiz, V. Dolz, L. Royo-Pascual, Advanced exergy analysis for a bottoming organic rankine cycle coupled to an internal combustion engine, Energy Convers. Manage. 126 (2016) 217–227, http://dx.doi.org/10.1016/j.enconman.2016.07.080.

[18] G. Liao, E. Jiaqiang, F. Zhang, J. Chen, E. Leng, Advanced exergy analysis for organic rankine cycle-based layout to recover waste heat of flue gas, Appl. Energy 266 (2020) 114891, http://dx.doi.org/10.1016/j.apenergy.2020.114891.

[19] M. Fallah, S.M. Mahmoudi, M. Yari, R. Akbarpour-Ghiasi, Advanced exergy analysis of the kalina cycle applied for low temperature enhanced geothermal system, Energy Convers. Manage. 108 (2016) 190–201, http://dx.doi.org/10.1016/j.enconman.2015.11.017.

[20] N. Yamankaradeniz, Thermodynamic performance assessments of a district heating system with geothermal by using advanced exergy analysis, Renew. Energy 85 (2016) 965–972, http://dx.doi.org/10.1016/j.renene.2015.07.035.

[21] A. Mortazavi, M. Ameri, Conventional and advanced exergy analysis of solar flat plate air collectors, Energy 142 (2018) 277–288, http://dx.doi.org/10.1016/j.energy.2017.10.035.

[22] F. Petrakopoulou, G. Tsatsaronis, T. Morosuk, A. Carassai, Conventional and advanced exergetic analyses applied to a combined cycle power plant, Energy 41 (2012) 146–152, http://dx.doi.org/10.1016/j.energy.2011.05.028.

[23] F. Chen, L. Liu, J. Peng, Y. Ge, H. Wu, W. Liu, Theoretical and experimental research on the thermal performance of ocean thermal energy conversion system using the rankine cycle mode, Energy 183 (2019) 497–503, http://dx.doi.org/10.1016/j.energy.2019.04.008.

[24] M.H. Sharqawy, J. Lienhard, S.M. Zubair, On exergy calculations of seawater with applications in desalination systems, Int. J. Therm. Sci. 50 (2011) 187–196, http://dx.doi.org/10.1016/j.ijthermalsci.2010.09.013.

[25] J.H. Anderson, Ocean thermal energy conversion (OTEC): choosing a working fluid, in: Proceedings of the ASME 2009 Power Conference POWER 2009, Vol. 81211, The Americal Society of Mechanical Engineering (ASME), 2009, http://dx.doi.org/10.1115/POWER2009-81211.

[26] F. Sinama, M. Martins, A. Journoud, A. Marc, F. Lucas, Thermodynamic analysis and optimization of a 10 MW OTEC Rankinecycle in Reunion Island with the equivalent Gibbs system method and generic optimization program GenOpt, Appl. Ocean Res. 53 (2015) 54–66, http://dx.doi.org/10.1016/j.apor.2015.07.006.

[27] S. Zhou, X. Liu, K. Zhang, Q. Yue, Y. Bian, S. Shen, Evaluation of a novel ammonia-water based combined cooling, desalination and power system based on thermodynamic and exergoeconomic analyses, Energy Convers. Manage. 239 (2021) 114176, http://dx.doi.org/10.1016/j.enconman.2021.114176.

[28] J. Wang, M. Diao, K. Yue, Optimization on pinch point temperature difference of ORC systembased on AHP-Entropy method, Energy 141 (2017) 97–107, http://dx.doi.org/10.1016/j.energy.2017.09.052.

[29] P. Ahmadi, I. Dincer, M. Rosen, Energy and exergy analyses of hydrogen production via solar-boosted ocean thermal energy conversion and PEM electrolysis, Int. J. Hydrogen Energy 38 (2013) 1795–1805, http://dx.doi.org/10.1016/j.ijhydene.2012.11.025.

[30] M.H. Sharqawy, J. Lienhard, S.M. Zubair, Thermophysical properties of seawater: a review of existing correlations and data, Desalination Water Treat. 16 (2010) 354–380, http://dx.doi.org/10.5004/dwt.2010.1079.

[31] S. Yousefizadeh-Dibazar, G. Salehi, A. Davarpanah, Comparison of exergy and advanced exergy analysis in three different organic rankine cycles, Processes 8 (2020) 586, http://dx.doi.org/10.3390/pr8050586.

[32] D. Colorado, Advanced exergy analysis applied to a single-stage heat transformer, Appl. Therm. Eng. 116 (2017) 584–596, http://dx.doi.org/10.1016/j.applthermaleng.2017.01.109.

[33] X. Wang, E.K. Levy, C. Pan, C.E. Romero, C. Banerjee, L. Pan, Working fluid selection for organic Rankine cycle power generation using hot produced supercritical CO_2 from a geothermal reservoir, Appl. Therm. Eng. 149 (2019) 1287–1304, http://dx.doi.org/10.1016/j.applthermaleng.2018.12.112.

[34] O. García-Valladares, P. Sánchez Upton, E. Santoyo, Numerical modeling of flow processes inside geothermal wells: An approach for predicting production characteristics with uncertainties, Energy Convers. Manage. 47 (2006) 1621–1643, http://dx.doi.org/10.1016/j.enconman.2005.08.006.

[35] G.C. Nihous, A preliminary assessment of ocean thermal energy conversion resources, J. Energy Resour. Technol. 129 (2007) 10–17, http://dx.doi.org/10.1115/1.2424965.

[36] D. Colorado, N. Demesa, A. Huicochea, J.A. Hernández, Irreversibility analysis of the absorption heat transformer coupled to a single effect evaporation process, Appl. Therm. Eng. 92 (2016) 71–80, http://dx.doi.org/10.1016/j.applthermaleng.2015.09.076.

[37] Y.R. Li, J.N. Wang, M.T. Du, S.Y. Wu, C. Liu, J.L. Xu, Effect of pinch point temperature difference on cost-effective performance of organic Rankine cycle, Int. J. Energy Res. 37 (2013) 1952–1962, http://dx.doi.org/10.1002/er.3105.

[38] M.H. Sharqawy, S.M. Zubair, J.H. Lienhard, Second law analysis of reverse osmosis desalination plants: An alternative design using pressure retarded osmosis, Energy 36 (2011) 6617–6626, http://dx.doi.org/10.1016/j.energy.2011.08.056.